Electronic Supplementary Material (ESI) for ChemComm.
This journal is © The Royal Society of Chemistry 2020

Supporting Information

Unravelling the Role of Active-site Isolation in Reactivity and Reaction Pathway Control for Acetylene Hydrogenation

Siyang Liu,‡[a,b] *Yiming Niu,*‡[b,c] *Yongzhao Wang,*[b,c] *Junnan Chen,*[b,c] *Xueping Quan,*[b] *Xia Zhang**[a] *and Bingsen Zhang**[b,c,d]

Experimental Section

Materials.

The multiwall CNTs (8–15 nm of outer diameter, 3–5 nm of inner diameter and 3–12 mm in length) were purchased from Shandong Dazhan nano materials Co., Ltd (China). Ethanol, hydrochloric acid and nitric acid were analytical grade (AG) and purchased from Sinopharm Chemical Reagent Co., Ltd (China). $Cu(NO_3)_2$ was purchased from Sinopharm Chemical Reagent Co., Ltd (China). $Pd(NO_3)_2$ was purchased from Adamas Reagent Co., Ltd.

Preparation of the Catalysts.

The oxidation of the multiwall CNTs. The original carbon nanotubes were stirred in concentrated hydrochloric acid at room temperature and refluxed with nitric acid at 120 °C, then washed with deionized water to acid-base neutral and thoroughly dried at 120 °C. The as-prepared sample is denoted as oCNTs. The uniform and abundant surface oxygen functional groups on the surface of oCNTs contribute to the homogeneous distribution of metal ions and the formation of Pd_xCu_y alloys.

The Pd_xCu_y/oCNTs catalysts were prepared by a simple impregnation-reduction method. The corresponding copper nitrate and palladium nitrate were dissolved in 0.1 M dilute nitric acid according to the atomic ratio and dispersed fully by ultrasound, then oCNTs were added into the mixed solution and stirred until they were fully mixed. The solvent was thoroughly removed by rotary evaporator and dried at 60 °C for 4 h, then reduced at 500 °C for 2 h in 50 vol.% H_2/Ar atmosphere, and cooled naturally to room temperature. According to the different atomic ratios of Pd to Cu, these catalysts are named as Pd_3Cu/oCNTs, Pd_2Cu/oCNTs, PdCu/oCNTs and $PdCu_3$/oCNTs, respectively.

For comparison, the Pd/oCNTs and Cu/oCNTs catalysts were prepared by the same method as the Pd_xCu_y/oCNTs catalysts. The loadings of above-mentioned catalysts are all 5 wt. %.

Catalyst Characterization.

Transmission Electron Microscopy

The high-angle annular dark-field scanning transmission electron microscopy (HAADF-STEM) images and energy dispersive X-ray spectroscopy (EDX) element maps for the Pd_xCu_y/oCNTs catalysts were acquired by FEI Tecnai G^2 F20 microscope. Before taking images, the powder sample was dispersed in ethanol solvent, and after being fully sonicated, it was dropped onto a 3 mm-diameter molybdenum grid covered with carbon film.

X-ray Diffraction

XRD patterns were obtained by Rigaku D/max 2400 diffractometer, which was operated at 40 kV, and equipped with a Cu Kα radiation source ($\lambda = 1.5418$ Å). The scanning angle (2θ) ranges from 10° to 80°.

X-ray Photoelectron Spectroscopy

The surface element composition and electronic structure of the catalysts were analysed by X-ray photoelectron spectrometer (ThermoFisher Science, ESCALAB250). The main parameters of the test: Al Kα (hv = 1489.6 eV) as the excitation source, the power is 150 W and the pass energy is 50.0 eV. The binding energy is calibrated by carbon (C1s = 284.6 eV).

Before the characterization, all the samples were reduced at 500°C for 2h in 50 vol.% H_2/Ar atmosphere.

Catalytic Performance

The selective hydrogenation reaction of acetylene was carried out in a fixed bed quartz tube reactor (diameter 12 mm) at atmospheric pressure. Ethylene-rich feedstock is adopted as reaction stream (0.504 vol.% acetylene, 5 vol.% hydrogen, and 20.11 vol.% ethylene, helium as balance). The Pd_xCu_y/oCNTs catalysts were diluted and added into the quartz reactor tube, and fixed in the constant temperature zone in the middle of the reactor. The Pd_xCu_y/oCNTs catalysts were in-situ reduced at 500°C for 2h in 50 vol.% H_2/He. When the catalysts were cooled to 200°C after reduction, the reaction stream with flow rate of 40 mL min^{-1} was introduced to start the test. Reaction products were analysed on-line by gas chromatography equipped with flame ionization detector (FID).

Calculation of the Conversion and Selectivity

The conversion of acetylene (C) was calculated by the formula as follow:

$$C = \frac{C_2H_2(in) - C_2H_2(out)}{C_2H_2(in)} \times 100\%$$

The selectivity of ethylene ($S_{C_2H_4}$) was calculated by the formula as follow:

$$S_{C_2H_4} = \left(1 - S_{C_2H_6} - S_{C_4H_8} - S_{C_4H_6}\right) \times 100\%$$

The selectivity of ethane ($S_{C_2H_6}$) was calculated by the formula as follow:

$$S_{C_2H_6} = \frac{C_2H_6(out) - C_2H_6(in)}{C_2H_2(in) - C_2H_2(out)} \times 100\%$$

The selectivity of butenes ($S_{C_4H_8}$) were calculated by the formula as follow:

$$S_{C_4H_8} = \frac{2 \times \left(C_4H_8(out) - C_4H_8(in)\right)}{C_2H_2(in) - C_2H_2(out)} \times 100\%$$

The selectivity of butadiene ($S_{C_4H_6}$) was calculated by the formula as follow:

$$S_{C_4H_6} = \frac{2 \times \left(C_4H_6(out) - C_4H_6(in)\right)}{C_2H_2(in) - C_2H_2(out)} \times 100\%$$

Calculation of the Mass specific activity and Mass specific yield

The mass specific activity was calculated by the formula as follow:

$$Mass\ specific\ activity = \frac{Space\ velocity(mmol/s)}{Active\ component\ mass(g)}$$

The mass specific yield was calculated by the formula as follow:

$$Mass\ specific\ yield = mass\ specific\ activity \times S_{C_2H_4}$$

Supplementary Figures

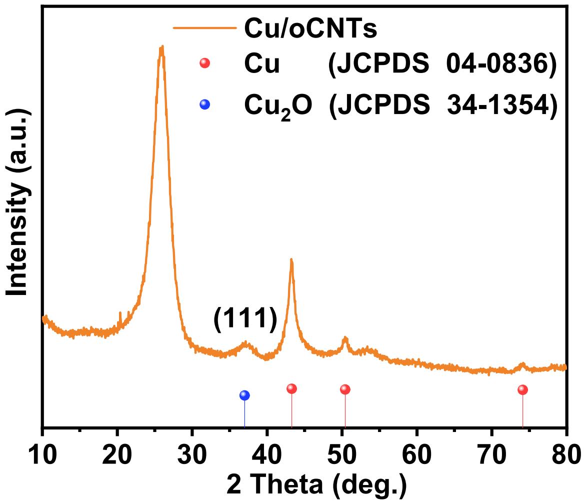

Figure S1. XRD pattern of Cu/oCNTs sample.

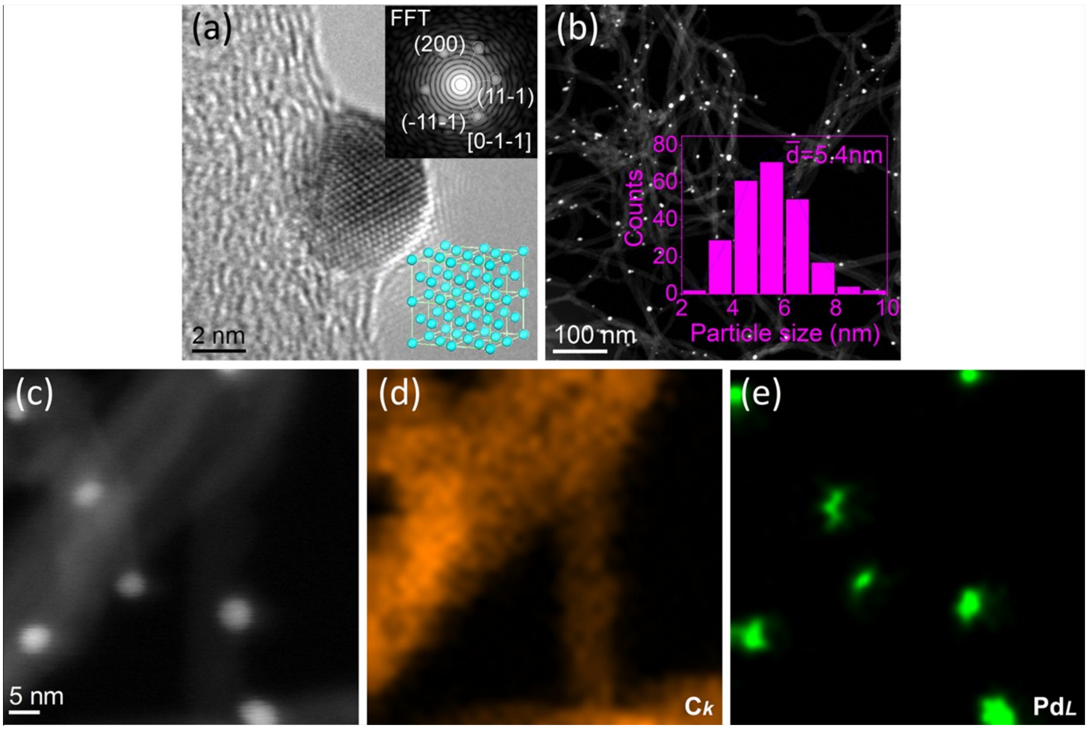

Figure S2. HRTEM (a) and HAADF-STEM (b) image of Pd/oCNTs sample, the insets in (a) and (b) are corresponding FFT, atomic model, and particle size histogram, respectively. (c-e) STEM image and corresponding EDX elemental maps of Pd/oCNTs.

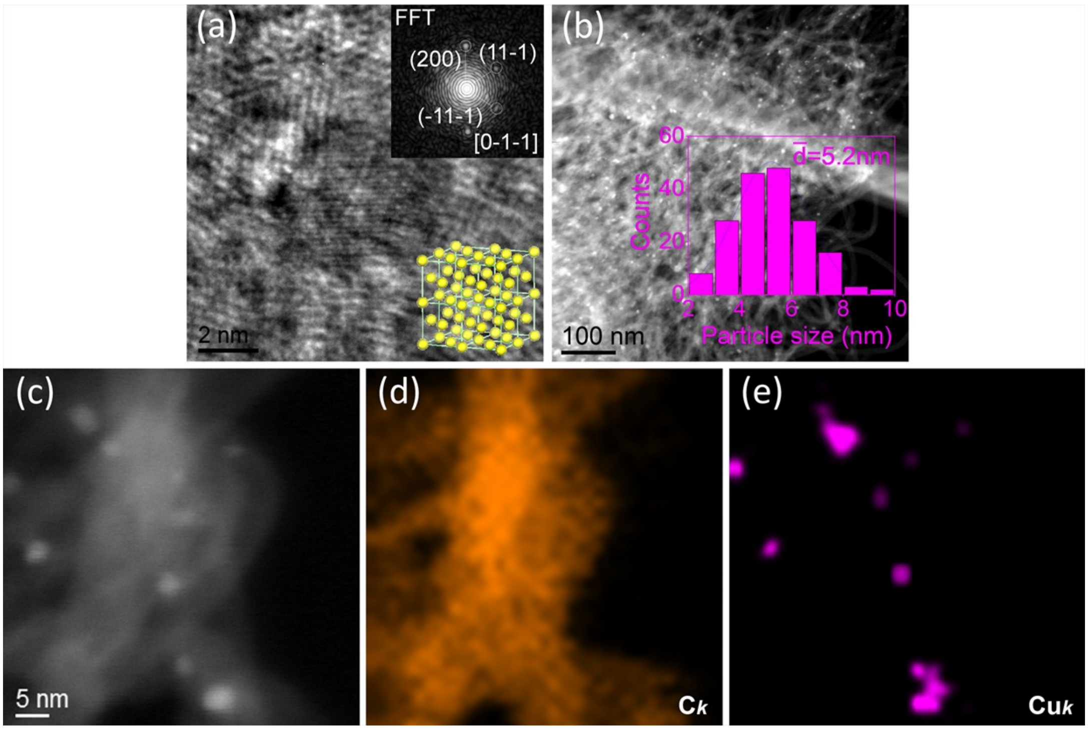

Figure S3. HRTEM (a) and HAADF-STEM (b) image of Cu/oCNTs sample, the insets in (a) and (b) are corresponding FFT, atomic model, and particle size histogram, respectively. (c-e) STEM image and corresponding EDX elemental maps of Cu/oCNTs.

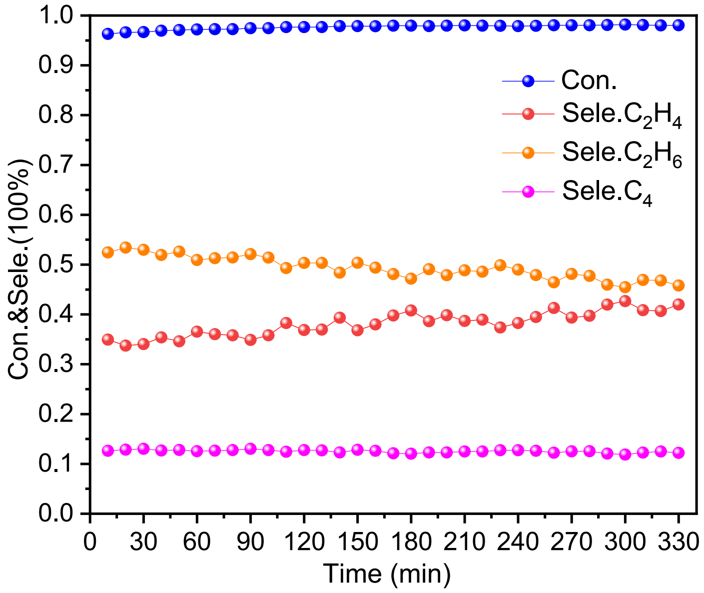

Figure S4. Ethylene, ethane, C_4 selectivity, and acetylene conversion as a function of time for Pd/oCNTs catalyst.

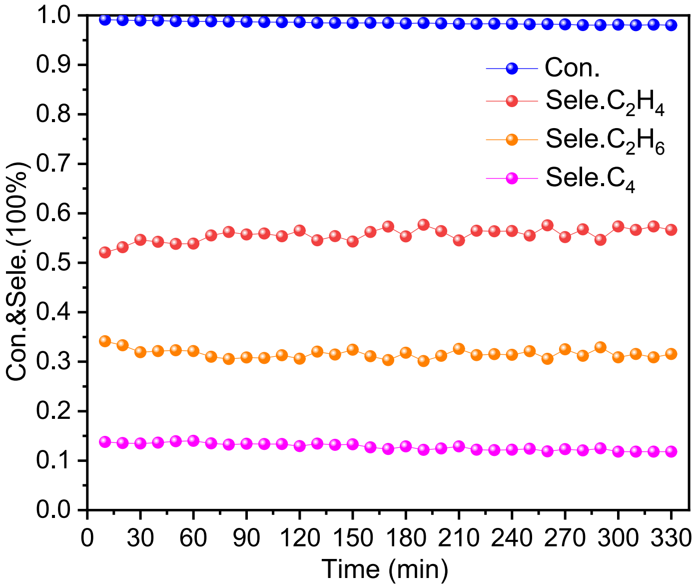

Figure S5. Ethylene, ethane, C_4 selectivity, and acetylene conversion as a function of time for Pd_3Cu/oCNTs catalyst.

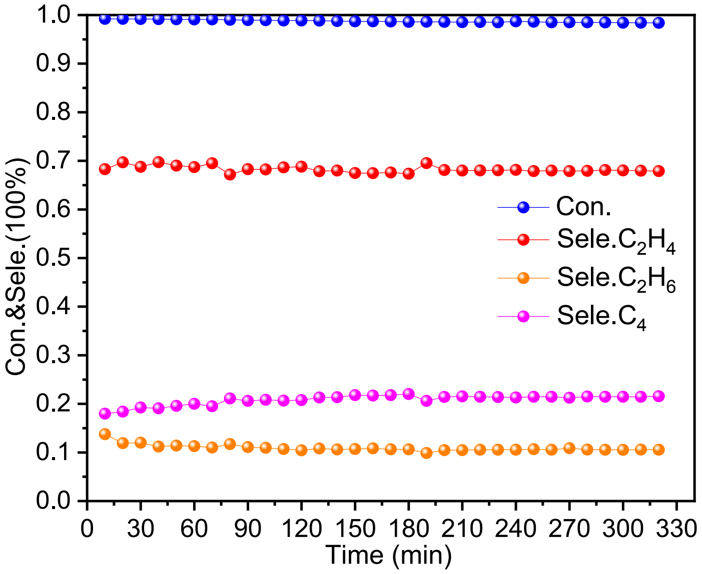

Figure S6. Ethylene, ethane, C_4 selectivity, and acetylene conversion as a function of time for Pd_2Cu/oCNTs catalyst.

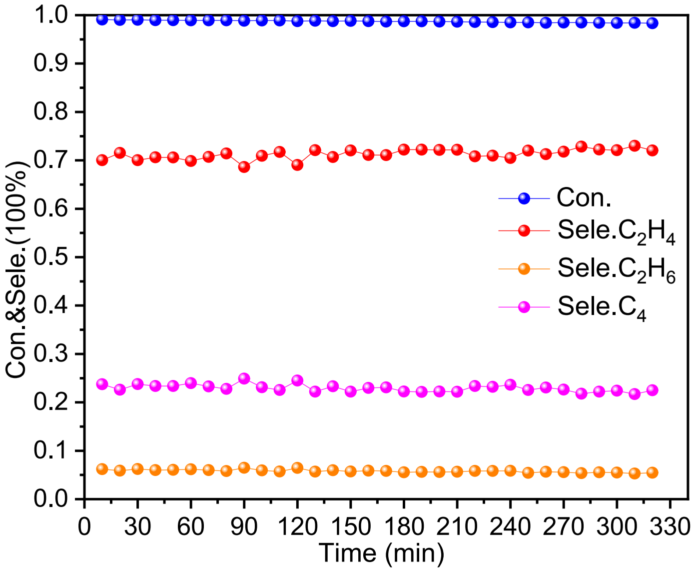

Figure S7. Ethylene, ethane, C_4 selectivity, and acetylene conversion as a function of time for PdCu/oCNTs catalyst.

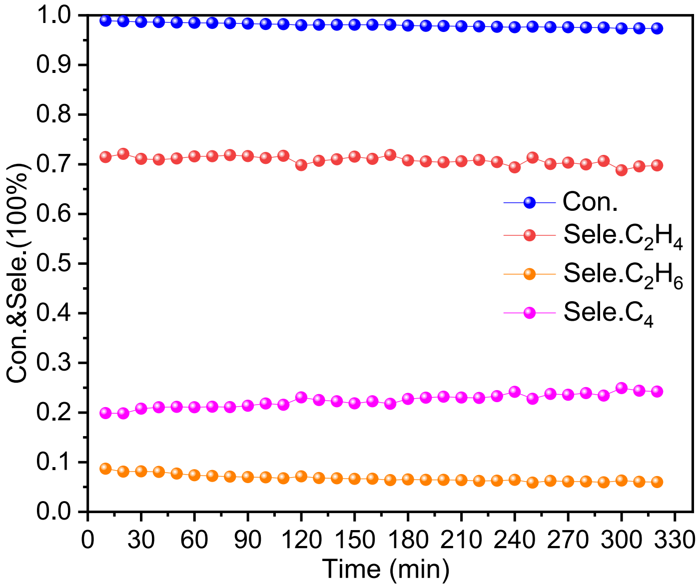

Figure S8. Ethylene, ethane, C_4 selectivity, and acetylene conversion as a function of time for $PdCu_3$/oCNTs catalyst.

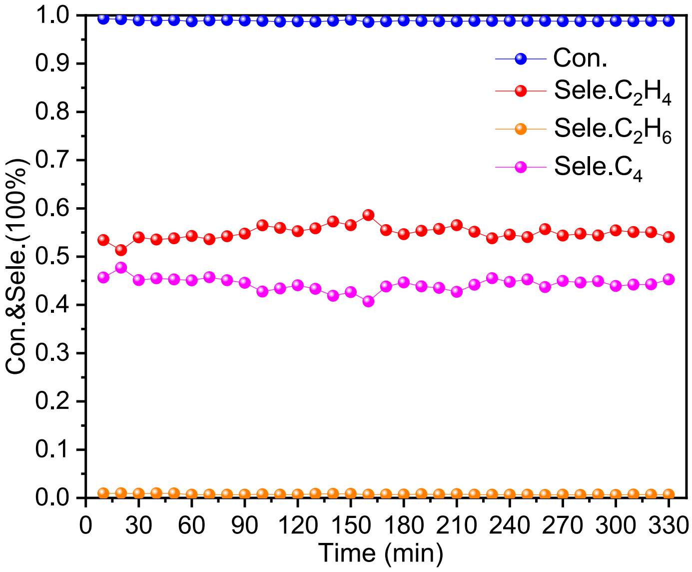

Figure S9. Ethylene, ethane, C_4 selectivity, and acetylene conversion as a function of time for Cu/oCNTs catalyst.

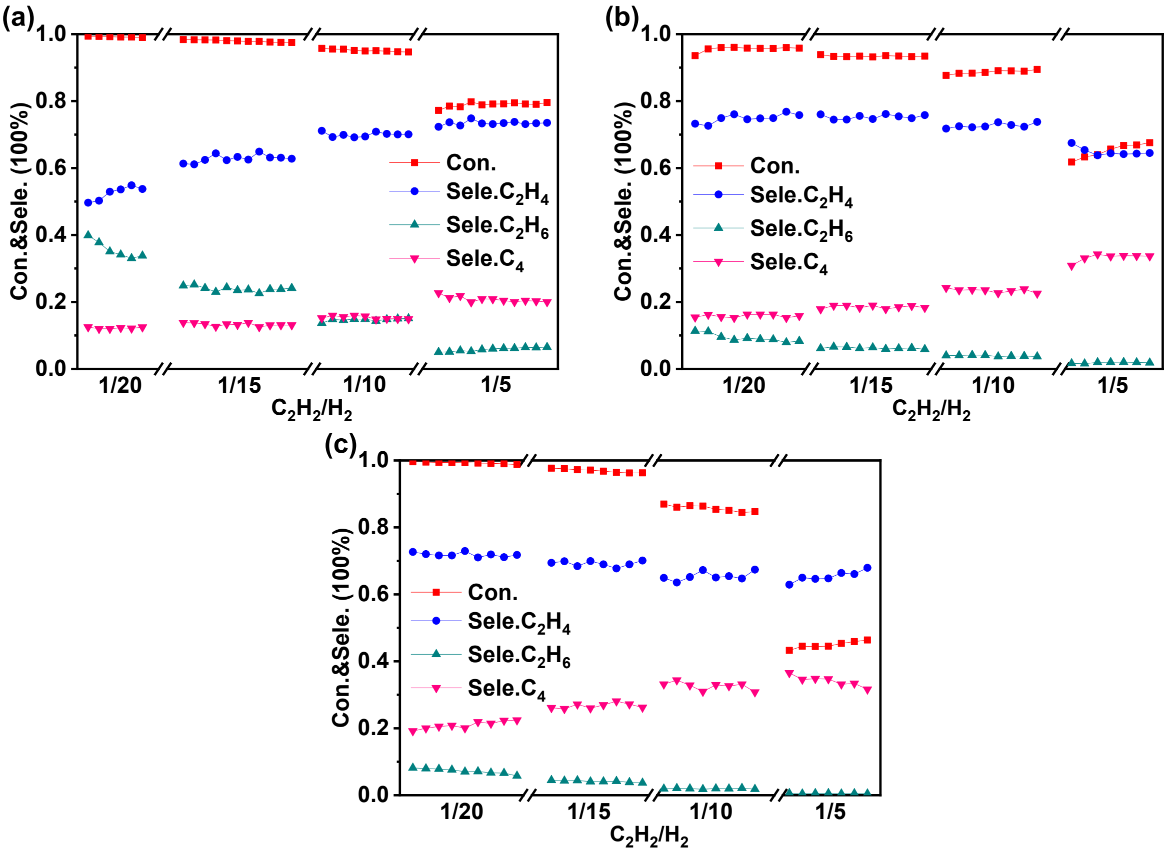

Figure S10. Catalytic performance of Pd$_x$Cu$_y$/oCNTs catalysts at different C$_2$H$_2$/H$_2$ ratios (1/20, 1/15, 1/10, and 1/5). (a) Pd$_3$Cu/oCNTs, (b) PdCu/oCNTs, and (c) PdCu$_3$/oCNTs.

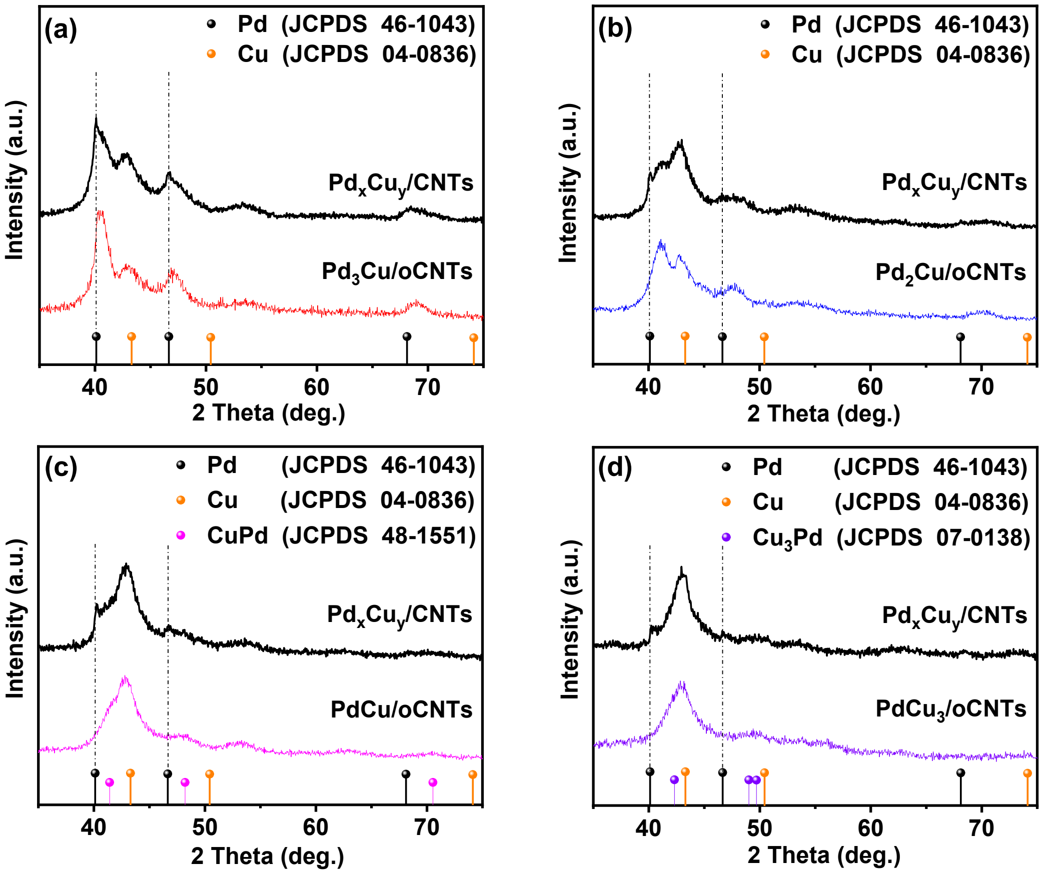

Figure S11. Comparison of Pd_xCu_y/oCNTs with failed synthesized samples. (a) Pd_3Cu/oCNTs, (b) Pd_2Cu/oCNTs, (c) PdCu/oCNTs, and (d) $PdCu_3$/oCNTs.

The CNTs with abundant oxygen functional groups exhibit superiority in homogeneous distribution of metal elements, which makes the formation of alloy NPs with uniform size and crystal structure accessible. If the oxygen functional groups on the surface are not well regulated, the resulting alloy NPs will not be uniform, as shown in Fig. S11.

Supplementary Table

Table S1. The quantitative analysis of XPS data.

Samples	**Theoretical Pd/Cu atomic ratio**	**Palladium content [at. %] [a]**	**Copper content [at. %] [a]**	**Pd/Cu atomic ratio**
Pd_3Cu/oCNTs	3/1	0.37	0.13	2.85
Pd_2Cu/oCNTs	2/1	0.3	0.12	2.5
PdCu/oCNTs	1/1	0.25	0.22	1.14
$PdCu_3$/oCNTs	1/3	0.21	0.3	0.7

[a] Determined by XPS

Table S2. Catalytic performance of Pd-based catalysts in acetylene hydrogenation.

Catalyst	**C_2H_2/H_2 (vol%)**	**Space velocity (mL g_{cat}^{-1} h^{-1})**	**Mass specific activity***	**Temp (℃)**	**Con (%)**	**Sele. C_2H_4 (%)**	**Sele. C_2H_6 (%)**	**Sele. C_4 (%)**	**Ref.**
Pd/oCNTs	0.5/5	$3{,}000\times10^4$	37.2	200	97.1	39	50	11	This work
Pd_3Cu/oCNTs	0.5/5	$2{,}400\times10^4$	35.7	200	98.5	55	32	13	
Pd_2Cu/oCNTs	0.5/5	$2{,}000\times10^4$	32.2	200	99.2	68	10	20	
PdCu/oCNTs	0.5/5	$1{,}200\times10^4$	23.8	200	98.8	72	6	22	
$PdCu_3$/oCNTs	0.5/5	480×10^4	16.6	200	98.5	71	6	23	
Cu/oCNTs	0.5/5	4.8×10^4	0.07	200	98.8	54	1	45	
Pd@C/CNT	0.5/3	6×10^4	0.25	150	90	70	-	-	Nanoscale 2017, 9, 14317
Pd/Gr	0.5/3	3×10^4	0.04	30	95	77	-	-	ChemCatChem 2017, 9, 3435
$Cu_{50}Pd/Al_2O_3$	0.6/1.8	GHSV 24,000 h^{-1}	-	100	100	71	6	23	Catal. Sci. Technol. 2015, 5, 2880
Au–Pd/SiO_2	1/5	60×10^4	4	65	45	39	55	6	Appl. Catal. A: Gen. 2014, 469, 419
Ag–Pd/SiO_2	1/5	60×10^4	4	65	70	50	42	8	
$Cu_{50}Pd/Al_2O_3$	0.6/1.8	GHSV 24,000 h^{-1}	-	100	99	70	8	22	J. Catal. 2015, 329, 538
PdCu/CNTs	1/5	632×10^4	0.8	70	70	60	30	10	Chem. Eur. J. 2019, 25, 8321
Pd-Zn/CNFs/SMFs	1.5/20	$1{,}740\times10^4$	32.4	140	15	80	10	10	J. Energy. Chem. 2013, 22, 717
$Cu_{60}Pd_{40}$	0.5/5	36×10^4	0.04	200	94	70	8	22	Materials 2013, 6, 2958
CoPd/MgO	0.5/1	15×10^4	0.93	150	80	41	54	5	J. Catal. 2013, 300, 125
Pd/CNTs-out	0.9/0.9	7500	0.09	110	100	68	23	9	Catal. Lett. 2014, 144, 2198
Pd/COP	0.6/0.9	152×10^4	0.19	120	99	75	12	13	ACS Catal. 2016, 6, 2435
Pd(Au)	1.2/2.2	GHSV 24,000 h^{-1}	-	90	100	53	6	41	Faraday Discuss. 2016, 188, 499
Pd-Ag/ZnO-Al_2O_3	1/2	3×10^4	0.4	90	100	77	6	17	Chin. J. Chem. 2017, 35, 1009

*: $mmol_{acetylene}\cdot g_{Pd}^{-1}\cdot s^{-1}$